

Constraints from Galileo observations on the origin of jovian dust streams

E. Grün*, M. Baguhl*, D. P. Hamilton†, R. Riemann*, H. A. Zook‡, S. Dermott§, H. Fechtig*, B. A. Gustafson§, M. S. Hanner||, M. Horányi¶, K. K. Khurana#, J. Kissel*, M. Kivelson#, B. A. Lindblad*, D. Linkert*, G. Linkert*, I. Mann**, J. A. M. McDonnell††, G. E. Morfill‡‡, C. Polanskey||, G. Schwehm§§ & R. Srama*

* Max-Planck-Institut für Kernphysik, 69117 Heidelberg, Germany

† University of Maryland, College Park, Maryland 20742-2421, USA

‡ NASA Johnson Space Center, Houston, Texas 77058, USA

§ University of Florida, Gainesville, Florida 32611, USA

|| Jet Propulsion Laboratory, Pasadena, California 91109, USA

¶ Laboratory for Atmospheric and Space Physics, University of Colorado, Boulder, Colorado 80309, USA

University of California at Los Angeles, Los Angeles, California 90024-1567, USA

* Lund Observatory, 221, Lund, Sweden

** Max-Planck-Institut für Aeronomie, 37191 Katlenburg-Lindau, Germany

†† University of Kent, Canterbury CT2 7NR, UK

‡‡ Max-Planck-Institut für Extraterrestrische Physik, 85740 Garching, Germany

§§ European Space Research and Technology Centre, 2200 AG Noordwijk, The Netherlands

THE *Ulysses* spacecraft detected streams of sub-micrometre-sized dust particles as it approached Jupiter in 1992^{1,2}. Although interplanetary space was known to contain dust, the presence of discrete streams was completely unexpected. The directions from which the dust grains struck the spacecraft strongly suggested that the source lay somewhere within the Jupiter system. Three origins were proposed, the comet Shoemaker–Levy 9 (ref. 3), Jupiter's gossamer ring⁴, and the volcanoes on Io⁵, but there was no definitive evidence for or against any of the options. Here we report the detection by the Galileo spacecraft of even more intense dust streams—including three intense dust storms of month-long duration, with impact rates up to 10 times higher than those observed by *Ulysses*. Our analysis of the data confirms that the dust streams originate near Jupiter; we are able to rule out a cometary origin, but cannot yet determine conclusively whether the dust comes from Io or the ring.

Galileo was launched in 1989, and followed a looping trajectory through the Solar System that brought it to Jupiter on 7 December 1995. The Galileo dust detector⁶, like its twin aboard *Ulysses*⁷, is an impact ionization detector which detects the plasma cloud released when a dust grain strikes its sensor. The impact direction (rotation angle) is determined by the spin position of the spacecraft at the time of impact, and both the impact speed and the mass of the dust grain can be derived from characteristics of the recorded charge pulses⁸. Normally these data are all transmitted to ground, but because Galileo relies on its low-gain antenna for communications and data transfer (its high-gain antenna failed to deploy), it cannot always transmit data in real time and must store it on-board. Because of limited memory aboard the spacecraft, some dust data is overwritten before it can be transmitted. Impacts are recorded in counters, but the complete information (from which the mass, velocity and direction are derived) is often lost. Thus for Galileo, we have two types of data: (1) impact rates and (2) information on individual dust impacts (impact charge, particle mass, relative velocity, impact time and impact direction).

In July 1994, the Galileo instrument was re-programmed to

improve its noise suppression capability; this increased its mass sensitivity by a factor of eight which is critical for studies of dust streams as these particles are very small. Figure 1a shows the rate of small impacts observed during the two years before Galileo's arrival at Jupiter. We call the three largest peaks dust 'storms' and the smaller peaks dust 'streams' and list relevant parameters in Table 1. The Galileo dust streams are similar in duration and intensity to the streams observed by *Ulysses*, although they do not display the one-month periodicity that the *Ulysses* streams did. Dust storms are an order of magnitude longer and more intense than dust streams. During the third and most intense dust storm, special campaigns were run by the Galileo operations team at the Jet Propulsion Laboratory that provided daily data transmissions and, in a special case (5 October 1995), hourly transmissions for 10 successive hours. These data showed that the impact rate fluctuated by up to a factor 100 over a day. No significant fluctuations have been found in the hourly sequence primarily because, at that time, the impact rate was low and statistical variations prevailed. No major changes were noted in the dust impact rate when Galileo crossed the bow shock in front of the jovian magnetosphere at the end of November.

Directional information on impacts is displayed in Fig. 1b. Impacts are separated in two ranges of impact charge. Small impacts are concentrated both in time and in direction (towards Jupiter). The threshold that effectively separates Jupiter dust-stream impacts from most of the rest of the impacts was apparent in the *Ulysses* data². Impact charges of dust-stream particles are most frequently very small, just above the detection threshold, suggesting even more numerous impacts with smaller amplitudes. Impact speeds range from 10 to 40 km s⁻¹ and masses range from 10⁻¹⁶ to 10⁻¹³ g. The true mass and speed values of the impacts may deviate significantly from those derived because the impact signals are both close to the threshold and at the edge of the calibrated range.

Zook *et al.*⁹ analysed *Ulysses* dust-stream measurements by taking into account both actual solar-wind plasma and magnetic-field data. They calculated dust trajectories between Jupiter and

BOX 1 Potential sources of jovian dust streams

(1) Comet Shoemaker–Levy 9³ (SL9)

Characteristics. Short-term dust emission during the June 1992 breakup of SL9 near Jupiter and the June 1994 impact of SL9 into the atmosphere of Jupiter. At an emission speed of 100 km s⁻¹ dust should have reached Galileo within 10 days of the impact.

Related observations. No coincidence between dust streams and main SL9 events: some streams occurred before and others long after these events.

(2) Jupiter's gossamer ring⁴

Characteristics. Continuous generation of ejecta from mutual collisions of ring particles, and from impacts of grains in the jovian system and interplanetary meteoroids. No fast source modulations. Modulations of the emitted dust intensity should occur only during the transit of the jovian magnetosphere and interplanetary space.

Related observations. Dust-stream activity is highly time variable, whereas Galileo measurements of the interplanetary magnetic field show little difference between the periods when a stream occurs and when no stream occurs.

(3) Volcanoes on Jupiter's satellite Io⁵

Characteristics. Time-variable dust emission correlated with volcanic activity. From Voyager observations of volcanic plumes a particle size range 0.001–0.01 μm was derived¹³. A dust production rate of 10⁵ to 10⁸ kg s⁻¹ is estimated.

Related observations. Dust-stream activity is highly time variable. Periodic stream activity was observed by *Ulysses*, but is not obvious in Galileo data. Because of lack of frequent Io observations, no correlation with volcanic activity has been identified.

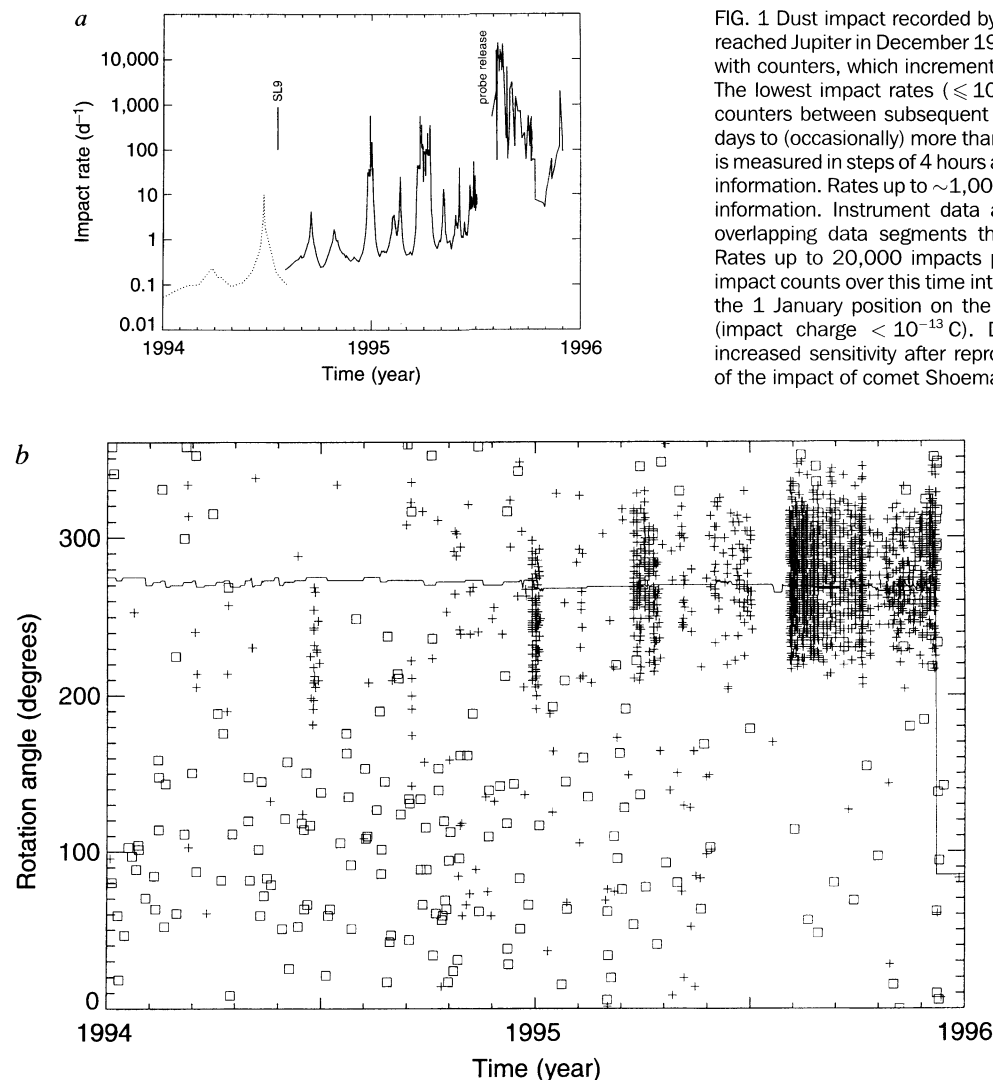


FIG. 1 Dust impact recorded by Galileo during the last two years before it reached Jupiter in December 1995. The instrument measures impact rates with counters, which increment from 0 to 255 over varying time intervals. The lowest impact rates ($\leq 100 \text{ d}^{-1}$) are determined from differences in counters between subsequent data transmissions, extending from a few days to (occasionally) more than a month. The time of an individual impact is measured in steps of 4 hours and is transmitted with the complete impact information. Rates up to $\sim 1,000$ impacts per day can be resolved from this information. Instrument data are transmitted to ground in two sets of overlapping data segments that are separated by about 20 minutes. Rates up to 20,000 impacts per day can be determined by comparing impact counts over this time interval. Note that year numbers are shown at the 1 January position on the horizontal axis. *a*, Rate of small impacts (impact charge $< 10^{-13} \text{ C}$). Dotted line, initial sensitivity; solid line, increased sensitivity after reprogramming the dust instrument. The time of the impact of comet Shoemaker-Levy 9 (SL9) onto Jupiter is indicated.

During July 1995, no data were received near the time of release of the atmospheric probe. *b*, Spacecraft rotation angles. Rotation angle is taken to be 0° when the dust-sensor axis points closest to the north ecliptic pole. At rotation angle 90° , the detector-axis points parallel to the ecliptic plane roughly in the direction of planetary motion. Impacts are marked according to their impact charges; crosses, $< 10^{-13} \text{ C}$; squares, $\geq 10^{-13} \text{ C}$. The rate of big impacts is about 0.4 d^{-1} and is only slowly varying¹⁴. The solid line indicates the direction to Jupiter. Data that include impact directions were obtained for only a small fraction of the impacts that occurred during dust storms.

TABLE 1 Parameters of the Jupiter dust streams observed by Galileo

Stream number	Centre of steam (date)	Distance to Jupiter (R_J)	Duration (d)	No. of counted impacts	No. of impacts with complete information
G1	25 June 94	3,500	8	22*	21
G2	16 Sept. 94	3,000	0.2	7	6
G3	1 Nov. 94	2,770	10	16	16
G4†	31 Dec. 94	2,390	10	~ 600	148
G5	7 Feb. 95	2,160	5	18	13
G6†	3 April 95	1,800	21	$\sim 1,000$	169
G7	5 May 95	1,600	12	26	21
G8	13 June 95	1,340	40	145	90
G9†	7 Sept. 95	755	80	$\sim 400,000$	1,131
G10	16 Nov. 95	220	20	$\sim 5,000$	51

All impacts were counted, but the complete information was received on the ground for only a small number of impacts (see text). Jupiter radius $R_J = 71.4 \times 10^3 \text{ km}$.

* Reduced sensitivity.

† Dust storm.

Ulysses that matched the observed impact directions, and argued that only very fast ($> 200 \text{ km s}^{-1}$) particles with a charge-to-mass ratio $\sim 1,000 \text{ C kg}^{-1}$ fit the Ulysses observations. Such a charge-to-mass ratio can only be reached by dust particles as small as $0.01 \mu\text{m}$ in radius. This size is about a factor of 10 below the size which we derived from the measured impact parameters and it implies that

Jupiter dust-stream particles are outside the calibrated mass and impact speed ranges.

Figure 2 top panel shows the mean spacecraft rotation angle of the instrument during the time of the dust storms. The mean rotation angle of the various impacts measures the out-of-ecliptic component of the dust velocity, the component that is most

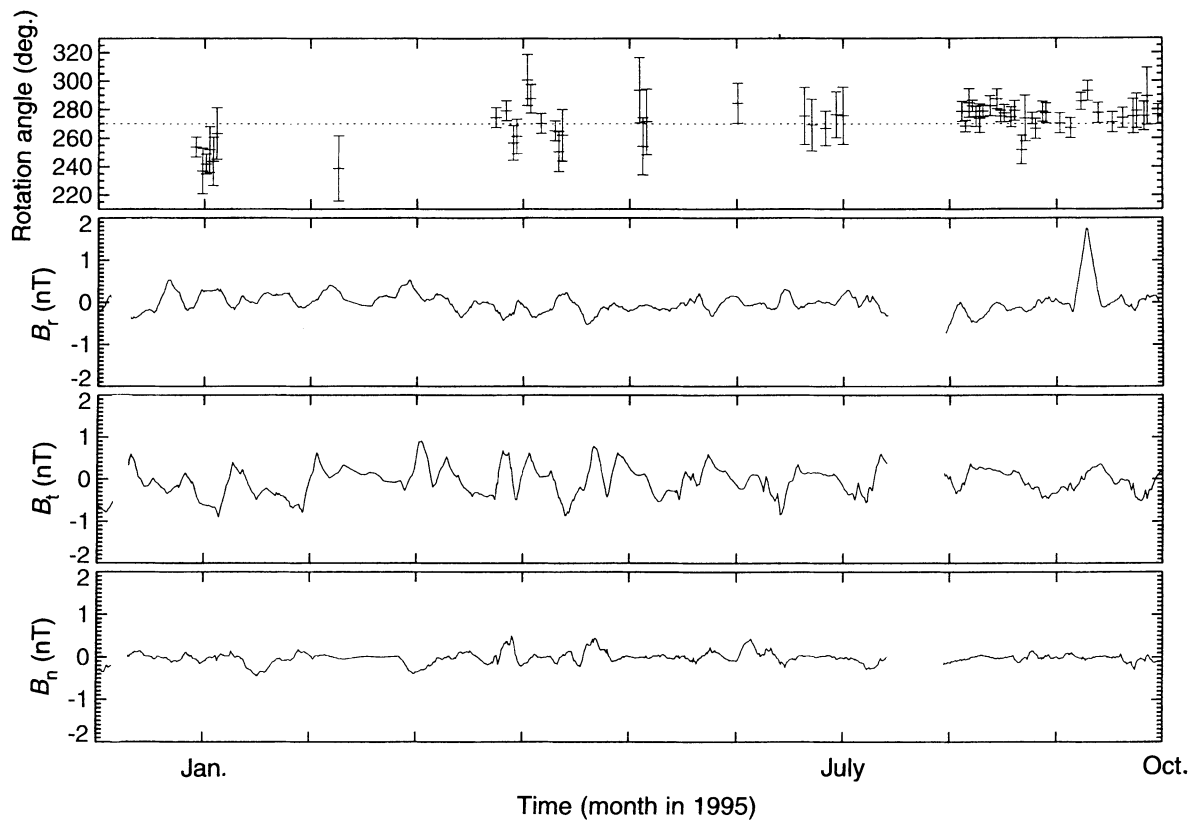


FIG. 2 Comparison of dust impact directions with magnetic field components over the period of the dust storms. Upper panel, mean spacecraft rotation angle of small dust impacts (impact charge $< 10^{-13}$ C) recorded during the time of the dust storms. The mean value is given whenever at least 4 impacts per day occurred. The dotted line indicates the direction to Jupiter. Lower panels, interplanetary magnetic field averaged over 4 days before the time given. The radial (with respect to the Sun), B_r , tangential, B_t , and normal (with respect to the solar equator), B_n , components are given. The data gap in July 1995 occurred when the atmospheric probe was released. Submicrometre-sized charged dust particles interact

with the interplanetary magnetic field via the Lorentz force which is perpendicular to both the velocity and the magnetic field vector. The velocity with which a dust particle travels relative to the magnetic field is roughly opposite to the solar-wind motion which carries this field away from the Sun. The dominant component of the interplanetary magnetic field in the outer Solar System is the tangential component, B_t , and, therefore, the Lorentz force acts predominantly away from or towards the solar equator (which is 7.3° off the ecliptic plane), that is, this force is directed approximately up- or downwards relative to the ecliptic plane (at rotation angles 90° and 270°).

affected by the tangential component of the interplanetary magnetic field. We show the average components of the magnetic field¹⁰ on the same timescale for comparison (Fig. 2 lower panels). The deviation of the rotation angle from the Jupiter direction resembles the fluctuations of the tangential magnetic field, B_t , around the zero value especially during the April storm. The magnetic field did not vary much during the time of the September storm, nor did the mean rotation angle of the dust particles. An accurate calculation of the interplanetary trajectories for the Galileo dust streams is underway.

Jupiter dust-stream activity seems to be highly time variable. The intensity varied by at least a factor of 1,000 between the weakest and the strongest streams observed by Galileo and Ulysses. Whereas streams recorded by Ulysses showed a periodicity of about 28 days, we do not find any correlation with this period in the Galileo data. Although the magnetic field was especially low during the last Galileo storm, the magnitude and variation was comparable to the magnetic field during the Ulysses post-flyby streams at other periods, for example, during the April storm.

Three potential dust sources have been discussed in the literature: the breakup and impact of comet Shoemaker–Levy 9³, Jupiter's gossamer ring⁴, and the volcanoes on Jupiter's satellite Io⁵. In Box 1 we show the characteristics of the three potential sources and discuss the relevant observations. Because of the missing coincidence of major stream activity with Shoemaker–

Levy 9 events, we rule out with high probability this comet as the cause for the dust streams. Despite the spectacular display of the comet impact itself, the production of dust capable of leaving the Jupiter system is most probably too low³ to make a significant contribution to dust-stream activity.

Observations of Jupiter's gossamer ring show that it consists mainly of micrometre-sized particles located in a disk between 1.8 and 3.0 jovian radii. Collisions among ring particles are common, and the submicrometre-sized products of these collisions are whisked away from Jupiter by powerful electromagnetic forces⁴. As this source produces a nearly steady flux of escaping particles, the periodicity in the Ulysses streams and the modulation of the Galileo streams would need to be effected solely by electromagnetic forces in the jovian magnetosphere and solar wind.

Sub-micrometre-sized dust produced during volcanic activity on Io⁵ can reach the jovian magnetosphere¹¹ and is subsequently ejected into interplanetary space by electromagnetic forces⁵. The dust production rate from Io's volcanic activity is assumed to be highly variable, and hence dust streams need not be modulated so strongly by electromagnetic forces. Unfortunately, observations of Io are still too sparse to establish or rule out a direct correlation between volcanic eruptions and dust-stream activity.

We conclude that the jovian ring and volcanoes on Io remain viable sources, but rule out dust from Shoemaker–Levy 9. More information on the temporal variation of dust streams and their source will be gained starting in July 1996, when we resume

receiving data from Galileo. In 2002, when the Cassini spacecraft flies by Jupiter *en route* to Saturn, we will get the first compositional measurements of the dust grains, which will provide more clues to their origin¹². □

Received 22 January; accepted 2 April 1996.

1. Grün, E. et al. *Nature* **362**, 428–430 (1993).
2. Baguhl, M., Grün, E., Linkert, G., Linkert, D. & Siddique, N. *Planet. Space Sci.* **41**, 1085–1098 (1993).
3. Grün, E. et al. *Geophys. Res. Lett.* **21**, 1035–1038 (1994).
4. Hamilton, D. P. & Burns, J. A. *Nature* **364**, 695–699 (1993).
5. Horányi, M., Morfill, G. E. & Grün, E. *Nature* **363**, 144–146 (1993); *J. Geophys. Res.* **98**, 21245–21251 (1993).

6. Grün, E. et al. *Space Sci. Rev.* **60**, 317–340 (1992).
7. Grün, E. et al. *Astr. Astrophys. Suppl.* **92**, 411–423 (1992).
8. Grün, E. et al. *Planet. Space Sci.* **43**, 941–951 (1995).
9. Zook, H. A. et al. in *Physics, Chemistry, and Dynamics of Interplanetary Dust* (eds Gustafson, B. A. S. & Hanner, M. S.) (Conf. Ser., Astr. Soc. Pacific, Provo, UT, in the press).
10. Kivelson, M. G., Khurana, K. K., Means, J. D., Russell, C. T. & Snare, R. C. *Space Sci. Rev.* **60**, 357–384 (1992).
11. Johnson, T. V., Morfill, G. E. & Grün, E. *Geophys. Res. Lett.* **7**, 305–308 (1980).
12. Srama, R., Grün, E. and the Cassini Dust Science Team in *Physics, Chemistry, and Dynamics of Interplanetary Dust* (eds Gustafson, B. A. S. & Hanner, M. S.) (Conf. Ser., Astr. Soc. Pacific, Provo, UT, in the press).
13. Collins, S. A. *J. Geophys. Res.* **86**, 8621–8626 (1981).
14. Baguhl, M. et al. *Space Sci. Rev.* **72**, 471–476 (1995).

ACKNOWLEDGEMENTS. We thank the Galileo operations team at JPL for their efficient cooperation and especially for the special campaigns that they provided. This work was supported by DARA.

Direct observation of a surface charge density wave

Joseph M. Carpinelli*, Hanno H. Weitering*,
E. Ward Plummer* & Roland Stumpf†

* Department of Physics and Astronomy, The University of Tennessee, Knoxville, Tennessee 37996, USA, and Solid State Division, Oak Ridge National Laboratory, Oak Ridge, Tennessee 37831, USA

† Sandia National Laboratory, Albuquerque, New Mexico 87185, USA

A CHARGE density wave (CDW) is a periodic symmetry-lowering redistribution of charge within a material, accompanied by a rearrangement of electronic bands (such that the total electronic energy is decreased) and usually a small periodic lattice distortion^{1,2}. This phenomenon is most commonly observed in crystals of reduced symmetry, such as quasi-two-dimensional³ or quasi-one-dimensional⁴ materials. In principle, the reduction of symmetry associated with surfaces and interfaces might also facilitate the formation of CDWs; although there is some indirect evidence for surface charge density waves^{5–12,14}, none has been observed directly. Here we report the observation and characterization of a reversible, temperature-induced CDW localized at the lead-coated (111) surface of a germanium crystal. The formation of this new phase is accompanied by significant periodic valence-charge redistribution, a pronounced lattice distortion and a metal–nonmetal transition. Theoretical calculations confirm that electron–phonon coupling drives the transition to the CDW, but it appears that some other factor—probably electron–electron correlations—is responsible for the ground-state stability of this phase.

Pb/Ge(111)- α consists of 1/3 monolayer of equivalent lead adatoms spaced $\sim 7\text{Å}$ apart in a hexagonal array of T_4 sites atop the bulk-truncated germanium lattice, forming the $(\sqrt{3} \times \sqrt{3})R30^\circ$ arrangement shown in Fig. 1. Clean, well ordered germanium (111) surfaces were first prepared in ultrahigh vacuum, followed by a room-temperature lead dose and subsequent anneal (at $\sim 250^\circ\text{C}$) to produce α -phase^{15–19}. Coverage was monitored with both low-energy electron diffraction (LEED) and Auger electron spectroscopy. In practice, some Ge adatom defects were always present in the overlayer.

We employed three experimental surface analysis techniques to characterize this thin film. LEED was used to determine the symmetry of the surface atomic lattice. Inelastic electron scattering (electron energy-loss spectroscopy (EELS)) was used to probe the excitation spectra of our interface. Scanning tunnelling microscopy (STM) was used to image the spatial variations in the surface charge density with atomic resolution²⁰.

We present first our results acquired at room temperature, where all previous investigations were performed^{15–19,21}. LEED data (Fig. 2a) include several sharp diffraction spots, characteristic of the $(\sqrt{3} \times \sqrt{3})R30^\circ$ surface symmetry displayed in Fig. 1. EELS data (Fig. 2a) indicate that the room-temperature α -phase

is metallic. This result is consistent with simple electron counting, where (based on the Pauli principle) two electrons from each unit cell sequentially populate the electronic bands (starting from low energy). In any geometry with an odd number of electrons per unit cell, the uppermost occupied band will be only partially filled, resulting in a metallic structure. The $(\sqrt{3} \times \sqrt{3})R30^\circ$ surface unit cell contains one lead atom (with a valency of four) and three outer layer germanium atoms (each with one unpaired electron), totalling seven valence electrons in all, and is therefore expected to be metallic. Figure 3a presents room-temperature STM data acquired in the same scan but at different bias voltages. In both the filled state and empty state, a hexagonal array of identical protrusions can be seen. The results of previous experiments¹⁸ and computer simulations¹⁹ indicate that each protrusion imaged is a lead adatom.

As the sample temperature is lowered, properties of the α -phase exhibit a dramatic change. For surfaces with a low enough defect density, the low-temperature LEED pattern now shows the presence of extra spots (Fig. 2b), characteristic of a new (3×3) symmetry. This transition in structure is gradual and reversible, with an onset near -20°C . EELS data of the low temperature α -phase are likewise very different from their room-temperature counterparts. There is no continuum of low energy losses; instead, a discrete loss onset can be seen, indicating a semiconducting interface. The inset of Fig. 2b shows similar data for a non-zero parallel momentum transfer (angle of reflection \neq angle of incidence) indicating more clearly the onset value. Whereas the room temperature α -phase is metallic, our observations indicate that a small band gap ($E_g \leq 0.065\text{V}$ at 100 K) evolves as tempera-

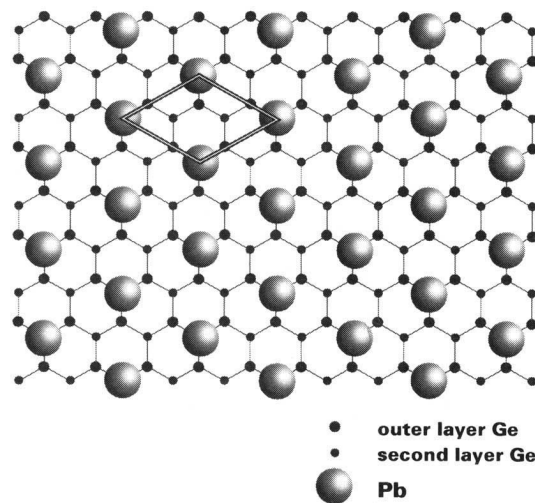


FIG. 1 Ball model of the α -phase of Pb/Ge(111); coverage is 1/3 monolayer. Lead adatoms are 7.0Å apart on T_4 sites atop the bulk truncated germanium lattice. The indicated unit cell shows the interface's $(\sqrt{3} \times \sqrt{3})R30^\circ$ symmetry (relative to the bulk truncated (1×1) symmetry).